Influence of charged walls and defects on DC resistivity and dielectric relaxation in Cu-Cl boracite

Cochard, Charlotte; Granzow, Torsten; Fernandez-Posada, C. M.; Carpenter, M. A.; McQuaid, Raymond G. P.; Guy, Joseph G. M.

Publication date:
2021

The following article has been submitted to Applied Physics Letters.

Influence of charged walls and defects on DC resistivity and dielectric relaxations in Cu-Cl boracite

C. Cochard,[1] T. Granzow,[2] C. M. Fernandez-Posada,[3] M. A. Carpenter,[3] R. G. P. McQuaid,[4] J. M. Guy,[4] R. W. Whatmore,[5] and J. M. Gregg[4]

[1)] *School of Science and Engineering, University of Dundee, Nethergate, Dundee, DD1 4HN, United Kingdom*[a)]

[2)] *MRT Department, Luxembourg Institute of Science and Technology (LIST), L-4362 Esch-sur-Alzette, Luxembourg*

[3)] *Department of Earth Sciences, University of Cambridge, Downing Street, Cambridge CB2 3EQ, United Kingdom*[b)]

[4)] *School of Mathematics and Physics, Queen's University Belfast, Belfast, BT7 1NN, United Kingdom*

[5)] *Department of Materials, Faculty of Engineering, Imperial College London, London, SW7 2AZ, United Kingdom*

(*Electronic mail: CCochard001@dundee.ac.uk)

(Dated: August 20, 2021)

Charged domain walls form spontaneously in Cu-Cl boracite on cooling through the phase transition. These walls exhibit changed conductivity compared to the bulk and motion consistent with the existence of negative capacitance. Here, we present the dielectric permittivity and DC resistivity of bulk Cu-Cl boracite as a function of temperature (-140 °C to 150 °C) and frequency (1 mHz to 10 MHz). The thermal behaviour of the two observed dielectric relaxations and the DC resistivity is discussed. We propose that the relaxations can be explained by the existence of point defects, most likely local complexes created by a change of valence of Cu and accompanying oxygen vacancies. In addition, the sudden change in resistivity seen at the phase transition suggests that conductive domain walls contribute significantly to the conductivity in the ferroelectric phase.

The boracites form a class of ferroelectrics with the general formula $M_3B_7O_{13}X$, where M is a metal and X a halide. As improper ferroelectrics, their interesting crystallography and phase transitions attracted attention in the 1960's, 70's and 80's with the first coupled magnetoelectric multiferroic switching being demonstrated by Ascher et al.[1] in $Ni_3B_7O_{13}I$ and with observations indicative of potential for electro-optic[2] and pyroelectric applications[3–5]. However, the growth of large single crystals[6,7] is difficult and with the development of perovskite oxide ceramic materials possessing diverse functional properties, interest in the boracite family subsequently waned. Recently, however, the discoveries surrounding improper ferroelectrics[8–10] and their associated charged domain walls[11,12] has rekindled interest in the potential of boracites as functional materials. The charged domain walls in Cu-Cl boracite are particularly remarkable: they present either enhanced conductivity (in 90° tail-to-tail walls) or reduced conductivity (in 90° head-to-head walls) relative to the bulk[12]. Charged walls exist spontaneously in Cu-Cl boracite, to accommodate for the spontaneous shear strain developing at the phase transition, but they can also be injected and repositioned by stress and electric field, making them interesting for the future of nanoelectronics[13,14]. Uniquely, head-to-head charged walls have been shown to have an unconventional electrostatic response (moving in the opposite direction to that expected under an applied electric field), consistent with the existence of negative capacitance[11]. This discovery of new properties at domain walls prompts our understanding of the intrinsic properties of boracites to be revisited.

The characterisation of the dielectric properties is particularly important, as it pertains to the unusual electrostatic response of charged domain walls[11], as well as playing a role in the piezoelectric and ferroelectric responses. Here, we focus on the characterisation of the dielectric dispersion and resistivity, as functions of temperature, of the same Cu-Cl boracite sample in which the conductivity of charged walls[12] and negative capacitance were measured[11]. We observe two dielectric relaxations and a strong change of resistivity at the phase transition (90°C) between the high-temperature piezoelectric phase and the low-temperature ferroelectric phase[15].

The $Cu_3B_7O_{13}Cl$ single-crystal was prepared by the phase transport technique[7]. The crystal is about 5x5x1mm^3. The sample is transparent with a faint blue coloration. The transmission spectrum of a small piece of the sample was measured on a PerkinElmer Lambda900 spectrometer between 300 nm and 900 nm. The impedance of this crystal was measured at frequencies between 1 mHz and 10 MHz in a large temperature range of -140 °C to 150 °C , spanning the piezoelectric-ferroelectric phase transition, with steps of 10 or 20 °C using a Novocontrol Concept 40 dielectric spectrometer with the unpoled sample directly contacted with parallel brass plates. The complex dielectric permittivity $\varepsilon^* = \varepsilon' + i\varepsilon''$ and resistivity $\rho^* = \rho' + i\rho''$ were calculated classically from the complex impedance.

Figure 1 presents the frequency dispersion of ε' and ε'' at different temperatures. Piezoelectric resonances are observed at frequencies above 500 kHz. With decreasing frequency, two relaxations can be clearly observed at frequencies around

[a)] Also at School of Mathematics and Physics, Queen's University Belfast, Belfast, BT7 1NN, United Kingdom.

[b)] Also at Maxwell Centre, Cavendish Laboratory, University of Cambridge, Cambridge, United Kingdom

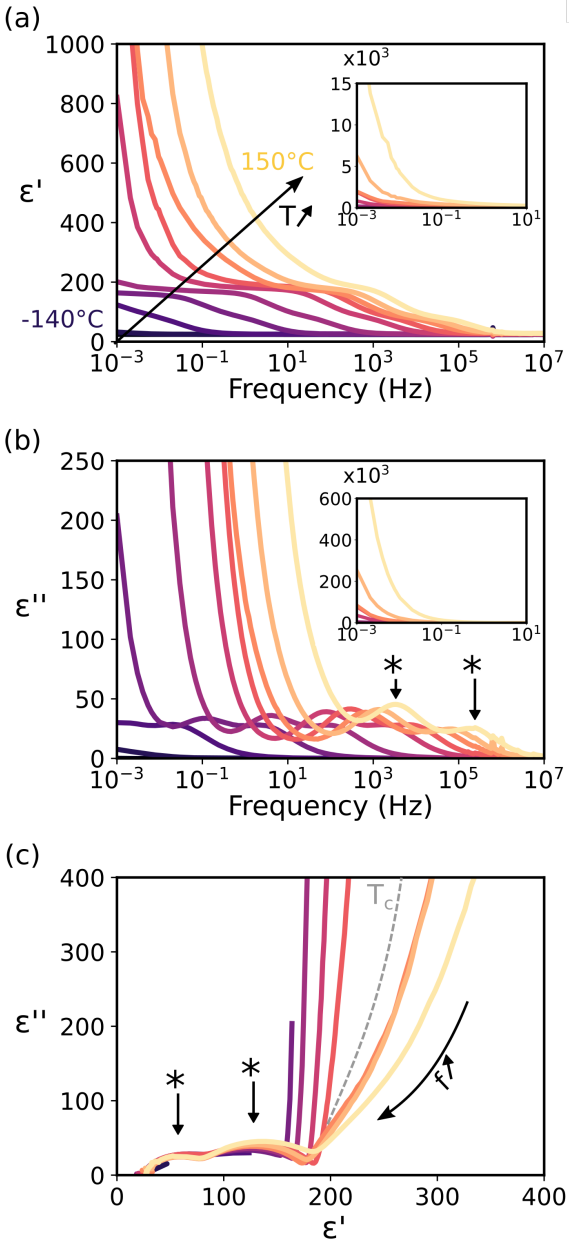

Figure 1. Frequency dependence of the dielectric permittivity (a) real part, (b) imaginary part and (c) Cole-Cole plot. * highlight the two relaxations in (b) and (c) The colour lines are separated by 20°C except close to the phase transition where they are separated by 10°C.

1 kHz and 100 kHz at 150 °C. Upon further lowering of frequencies, the real and imaginary parts of the dielelectric permittivity increase rapidly. This increase is consistent with the existence of a resistor in series. The real and imaginary part were fitted simultaneously for frequencies below piezoelectric resonances for all temperatures. The relaxations were modelled with the Debye function, and a term was added to describe the low-frequency conductive behaviour, as is commonly done in ferroelectric materials[16]

$$\varepsilon^* = \frac{\Delta\varepsilon_1}{1+i(f/f_{r,1})} + \frac{\Delta\varepsilon_2}{1+i(f/f_{r,2})} + \frac{\sigma}{\varepsilon_0(i2\pi f)^n} + \varepsilon_\infty \quad (1)$$

where $\Delta\varepsilon_1$ and $\Delta\varepsilon_2$ are the amplitudes of the relaxations, $f_{r,1}$ and $f_{r,2}$ the two characteristic relaxation frequencies, σ is the DC conductivity, n is an empirical constant and ε_∞ is the permittivity at high frequencies. Fitting the two relaxations with the empirical Havriliak-Negami function[17] slightly improves the quality of the fit, but does not change the amplitudes and the frequencies of the fit (Supplementary Fig. 5). The fitting parameters for the two relaxations, on the one hand, and the DC conductivity, on the other hand, are presented in Fig. 2 and Fig. 3, respectively, and will be discussed separately.

Figure 2 presents the fitted parameters for the two relaxations. Both relaxations have similar thermal evolution: the relaxation frequencies (Fig. 2a) continuously increase with increasing temperature and the amplitudes of the two relaxations display a sudden jump at the phase transition. The temperature evolution of relaxation frequencies is often modelled using the Vogel-Fulcher law, describing an activated process of activation energy E_a and freezing below the temperature T_f

$$f = f_0 e^{-\frac{E_a}{k_B(T-T_f)}} \quad (2)$$

where k_B is the Boltzmann constant and f_0 the attempt frequency. The continuous lines in Fig. 2(a) represent the results of the fit to the measured data. Fitting a Vogel-Fulcher law is never trivial[18], but a few things can be said based on the fitted values shown in Table I.

The freezing temperatures were found to be ~ 0 K (within error), suggesting that the processes leading to the relaxations will not freeze. Fixing the freezing temperature to 0 K, i.e. assuming an Arrhenius law, leads to similar results with activation energies that are slightly smaller, but still within the error associated with the Vogel-Fulcher fits.

A recent study[15], focusing on the elastic properties of this sample, identified a relaxation process freezing at ~ 40 K, which was attributed to strain relaxation around local ferroelectric dipoles or polarons. The low freezing temperature observed could be broadly consistent with our observations; however, the activation energy (~ 0.02 eV) associated with the strain process is more than an order of magnitude lower than that observed in this work. The differences in activation energies and freezing behaviour suggest different microscopic origins for the relaxation processes reported in the present work and the one previously observed. Specifically, the absence of freezing of the relaxation observed here suggests that the reorientations of local dipoles are independent. Indeed, in a process modelled by an Arrhenius law, there is no assumption of collective response to the applied electric field.

Notably, the activations energies for both relaxations are the same within error (~ 0.6 eV). This suggests a common origin. Domain wall motion can largely be excluded, as both relaxation phenomena persist above T_c. While a contribution from domains/domain walls below T_c cannot be completely excluded, it is certainly not the main relaxation phenomenon at play.

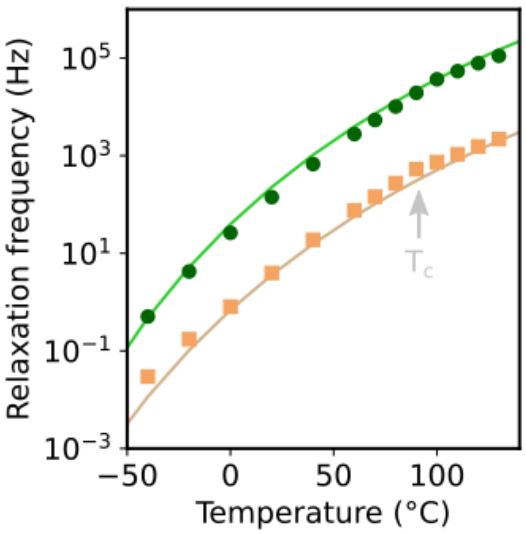

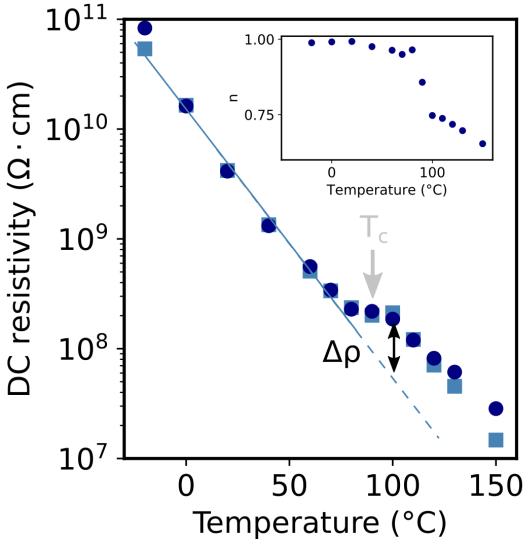

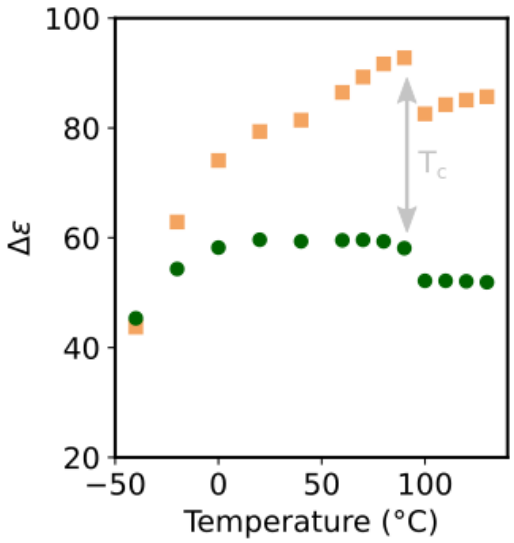

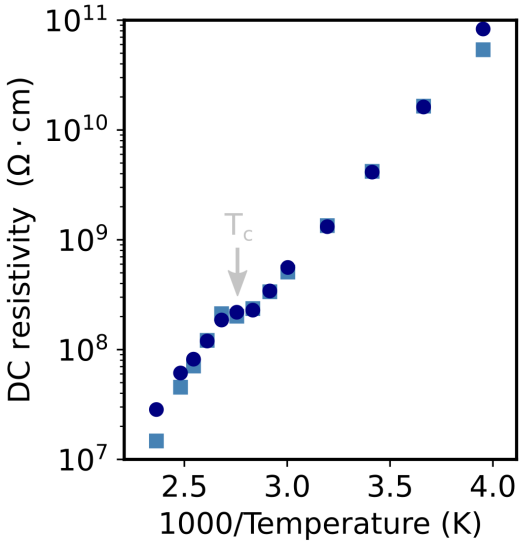

Figure 2. Fitting parameters of relaxations (a) relaxation frequency, (b) dielectric strength. The dark green circles represent the high frequency relaxation and the light orange squares the lower frequency one.

Figure 3. Thermal evolution of resistivity (a) as a function of temperature (b) as a function of the inverse of temperature. Light blue squares represent the value of resistivity measured at 1mHz. Dark blue circles depict the value obtained from the fitting procedure. The exponent n is presented in the inset of (a).

Table I. Fitting parameters of the Vogel-Fulcher analysis. Relaxation 1 and 2 correspond to the relaxation occurring at the highest and lowest frequency, respectively.

	T_f	E_a (eV)	f_0 (Hz)
Relaxation 1	-5 ± 9	0.63 ± 0.04	$(7.7 \pm 4.0) \cdot 10^{12}$
Relaxation 2	-12 ± 11	0.62 ± 0.05	$(9.4 \pm 6.2) \cdot 10^{12}$

Perhaps the most classical origin of dielectric relaxations in dielectrics, point defects[19–21] are the most likely mechanism for the observed dielectric relaxations. Indeed, the order of magnitude of the activation energies is very similar to that reported for defect states in perovskites[22]. UV-visible optical spectroscopy (Fig. 4) indicates the existence of states in

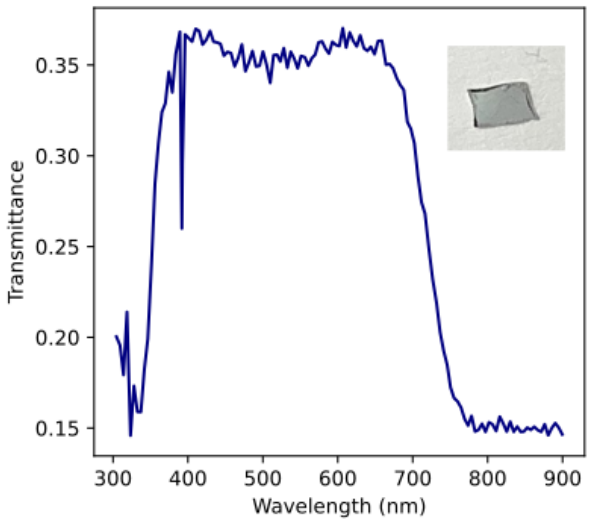

Figure 4. Transmittance of the Cu-Cl boracite sample (photo as inset)

the band gap, strongly supporting point defects as a source of the dielectric relaxations. The colour of the sample and the band in the transmission spectrum at 490-540nm[23] both suggest a change of valence of copper $Cu^{2+} \rightarrow Cu^{+}$. To conserve charge neutrality, this change of valence is likely to be associated with positively charged point defects, such as oxygen vacancies $V_O^{\bullet\bullet}$.

Point defects can lead to dielectric relaxation in several ways: creating a local dipole (or bound charge) that can be reoriented by the electric field or providing a free charge carrier that is moved by the electric field. In parenthesis, defect mobility leads to dielectric relaxations in some cases, but have usually much higher activation energies ($\sim 2\,$eV in boracite glass[24]) and are rarely observed in ferroelectrics around room temperature. The similar activation energies suggest that the two relaxations "experience" a similar energy landscape. On the other hand, the difference in f_0 indicates that, at infinite temperature, the energy barrier between the minima is overcome at different frequencies. This could be explained with different effective masses of the dipoles or charges.

For example, the change of valence in copper creates a local dipole but can also lead to polaronic hopping between sites. These two mechanisms would probably have similar energy landscapes, but the dipole reorientation and polaron hopping would have different effective masses. Alternatively, the existence of anisotropy in some of the B-O tetrahedra could create relaxations with different effective masses. Indeed, in half of the tetrahedra, boron is not located at the centre. This off-centring leads to the existence of local dipoles (even in the high temperature phase) pointing towards chlorine. The position of a $V_O^{\bullet\bullet}$ vacancy would have a strong influence on this local B-O dipole and in turn change the effective mass of the dipole created directly by $V_O^{\bullet\bullet}$. A third option would be a defect complex formed of Cu^{+} and $V_O^{\bullet\bullet}$; this seems particularly likely, in terms of keeping the electroneutrality of the sample. This complex would have one activation energy, but the Cu^{+}- dipoles and $V_O^{\bullet\bullet}$ would again have different effective masses. By analogy with acceptor- or donor-doped perovskite[25,26] and the observed decrease in formation energy when a defect complex is created[27,28], we believe that a charge transfer between the two defects is the most likely phenomenon.

Below the frequencies of the dielectric relaxations, a strong increase in both ε' and ε'' is observed. It is attributed to the DC conductivity of the sample, which can be determined in two different ways: (i) as a result of fitting equation (1) to the dielectric dispersion data and (ii) considering the low-frequency (1 mHz) value of the resistivity ρ (Supplementary Figure 6a). Figure 3 presents the thermal behaviour of resistivity determined both ways. The values are in excellent agreement and are of the order of magnitude of the highest resistivity previously reported in Cu-Cl boracite[29], which suggests good reliability of our data.

At the phase transition, a clear jump in resistivity ($\Delta\rho$) of about an order of magnitude is observed. A similar step was seen in the exponent n, determined in the fitting procedure (see inset of Fig. 3(a)). This abrupt change is not an artefact, since it can be observed directly on the Cole-Cole plot (Fig. 1c): there is a clear and sudden change in the low frequency impedance across the phase transition. Schmid and Petermann[29] also reported a sudden change in resistivity at the phase transition, although they observed that the sign of $\Delta\rho$ depended on the sample and the poling state. This led the authors, in 1977, to conclude that "this may possibly be due to some spurious domain orientation [...] or to a higher conduction along the walls", even though domain wall conduction had not been experimentally observed in any ferroelectric system at that time. We observed a similar influence of the domain pattern in the DC resistivity measured at room temperature for the same sample after different thermal treatment (Supplementary Fig. 6b and Fig. 7): the highest resistivity being more than twice as large as the smallest one. However, now that enhanced or depressed conduction at domain walls[11,12] has been previously observed experimentally through spatially resolved current mapping, it is more likely that the domain walls influence predominantly the DC resistivity rather than "spurious domains", since single domains samples consistently show higher resistivity than multidomain ones[29].

In addition to its abrupt change at the phase transition, the DC resistivity decreases with increasing temperature, which indicates an insulator/semiconductor behaviour. It is common to study the temperature dependence to get insight into the physical mechanism responsible for carrier transport. In this work, two temperature dependences were considered: (i) increase in the number of charged carriers, due to the temperature dependence of the Fermi-Dirac function and (ii) activated hopping between potential wells described as follows

$$\text{(i)} \quad \rho_{DC} = \rho_0 e^{-\alpha T} \quad \text{and} \quad \text{(ii)} \quad \rho_{DC} = \rho_0 e^{\frac{E_a}{k_B T}}$$

where ρ_0 is a prefactor representing either the resistivity at T=0 K (i) or at infinite temperature (ii), α is a growth con-

stant, E_a the activation energy and k_B the Boltzmann constant. The description based on activated temperature dependence is more commonly used for dielectrics than that assuming intrinsic semiconductor behaviour, since defects are often the source of the DC conductivity. In the present case, the change in conductivity observed at charged walls could lead to an increase in the free charge carrier density with increasing temperature, hence suggesting a more intrinsic semiconductor behaviour[30–32]. This is particularly pertinent since the disappearance of domains at the phase transitions is accompanied with an abrupt change in resistivity.

Both models of resistivity were fitted as the logarithm of resistivity. The growth constant was fitted to a value $\alpha = 0.05 \pm 0.005\,\mathrm{K}^{-1}$ above and below the phase transition, while the activation energies were found to differ on each side of the phase transition with $E_a = 0.42 \pm 0.04\,\mathrm{eV}$ below and $E_a = 0.72 \pm 0.08\,\mathrm{eV}$ above the transition, respectively. These values of activation energies are of the same order of magnitude as the values reported in the literature for Cu-Cl boracite, although we observe the higher activation energy above T_C. Additionally, they are also of the same order as the one reported for the temperature dependence of the electronic conductivity driven by charge transfer between Cu^+ and Cu^{2+} in a halide double perovskite[33]. Both fits give reasonably good agreement factors, making it difficult to draw conclusions regarding the most likely physical mechanism for the change in DC conductivity. One the one hand, with an optical bandgap larger than 4 eV and the observation of defect states in the band gap, defect-mediated charge transport could seem to be the more likely mechanism for the observed thermal evolution of the resistivity. On the other hand, below the phase transition, charged domain walls were shown to play an important role in the resistivity of the sample. We hypothesize that below the phase transition, both defects and charged domain walls contribute to the resistivity. In this case, the apparent reduction in activation energy that would not be expected for the sole contribution of point defects would stem from the domain wall contribution.

In summary, the impedance spectra of Cu-Cl boracite were measured at different temperatures. Two dielectric relaxations and an increase of permittivity at low frequencies, consistent with the existence of a series resistor, were found. The study of the temperature evolution of the two relaxations and the low-frequency conductivity revealed the role of point defects. Based on the similarity of activation energies ($\sim 0.6\,\mathrm{eV}$) and differences in attempt frequencies ($f_0 = 7 - 9 \cdot 10^{12}\,\mathrm{Hz}$), we suggest that defect complexes, related to a change of valence of Cu and oxygen vacancies, are the most likely. Below the ferroelectric phase transition temperature, a decrease in resistivity is observed, consistent with the appearance of the conductive domain walls known in this system.

SUPPLEMENTARY MATERIAL

See supplementary material for the difference between Debye and Havriliak-Negami fitting, the effect of thermal treatment on the complex dielectric permittivity and the resistivity dispersion.

ACKNOWLEDGMENTS

The assistance of C. J. Brierley at Plessey Research (Caswell) Ltd. in growing the boracite crystals is gratefully acknowledged. The authors acknowledge funding from the Engineering and Physical Sciences Research Council (EPSRC: EP/P02453X/1; EP/P020194/1), the US-Ireland Research and Development Partnership Programme (USI 120)

DATA AVAILABILITY STATEMENT

The data that support the findings of this study are available from the corresponding author upon reasonable request.

REFERENCES

[1] E. Ascher, H. Rieder, H. Schmid, and H. Stössel, "Some Properties of Ferromagnetoelectric Nickel-Iodine Boracite, $Ni_3B_7O_{13}I$," Journal of Applied Physics **37**, 1404–1405 (1966).
[2] H. Schmid and J. Schwarzmüller, "Review of Ferroelectric Materials Usable for Passive Electro-Optic Alphanumeric Display Devices," Ferroelectrics **10**, 283–293 (1976).
[3] H. Schmid, P. Genequand, G. Pouilly, and P. Chan, "Pyroelectricity of Fe-I and Cu-Cl boracite," Ferroelectrics **25**, 539–542 (1980).
[4] W. A. Smith, M. E. Rosar, and A. Shaulov, "Analysis of pyroelectric and dielectric measurements on boracites," Ferroelectrics **36**, 467–470 (1981).
[5] R. W. Whatmore, J. M. Herbert, and F. W. Ainger, "Recent developments in ferroelectrics for infrared detectors," Physica Status Solidi (a) **61**, 73–80 (1980).
[6] H. Schmid, "Die synthese von boraziten mit hilfe chemischer transportreaktionen," Journal of Physics and Chemistry of Solids **26**, 973–976 (1965).
[7] R. W. Whatmore, C. J. Brierley, and F. W. Ainger, "Nucleation control during the growth of boracite single crystals," Ferroelectrics **28**, 329–332 (1980).
[8] G. Catalan, J. Seidel, R. Ramesh, and J. Scott, "Domain wall nanoelectronics," Reviews of Modern Physics **84**, 119–156 (2012).
[9] D. M. Evans, C. Cochard, R. G. P. McQuaid, A. Cano, J. M. Gregg, and D. Meier, "Improper Ferroelectric Domain Walls," in *Domain Walls* (Oxford University Press, 2020) p. 129–151.
[10] J. S. Feng, K. Xu, L. Bellaiche, and H. J. Xiang, "Designing switchable near room-temperature multiferroics via the discovery of a novel magnetoelectric coupling," New Journal of Physics **20**, 053025 (2018).
[11] J. G. Guy, C. Cochard, P. Aguado-Puente, E. Soergel, R. W. Whatmore, M. Conroy, K. Moore, E. Courtney, A. Harvey, U. Bangert, A. Kumar, R. G. McQuaid, and J. M. Gregg, "Anomalous Motion of Charged Domain Walls and Associated Negative Capacitance in Copper–Chlorine Boracite," Advanced Materials **33**, 2008068 (2021).
[12] R. G. McQuaid, M. P. Campbell, R. W. Whatmore, A. Kumar, and J. M. Gregg, "Injection and controlled motion of conducting domain walls in improper ferroelectric Cu-Cl boracite," Nature Communications **8**, 15105 (2017).
[13] J. Seidel, "Domain walls as nanoscale functional elements," Journal of Physical Chemistry Letters **3**, 2905–2909 (2012).
[14] J. R. Whyte and J. M. Gregg, "A diode for ferroelectric domain-wall motion," Nature Communications **6**, 1–5 (2015).
[15] C. M. Fernandez-Posada, C. Cochard, J. M. Gregg, R. W. Whatmore, and M. A. Carpenter, "Order–disorder, ferroelasticity and mobility of domain walls in multiferroic Cu–Cl boracite," Journal of Physics: Condensed Matter **33**, 095402 (2021).
[16] T. Granzow, "Polaron-mediated low-frequency dielectric anomaly in reduced $LiNbO_3$:Ti," Applied Physics Letters **111**, 022903 (2017).

[17]S. Havriliak and S. Negami, "A complex plane representation of dielectric and mechanical relaxation processes in some polymers," Polymer **8**, 161–210 (1967).

[18]C. Cochard, X. Bril, O. Guedes, and P.-E. Janolin, "Interpretation of Polar Orders Based on Electric Characterizations: Example of $Pb(Yb_{1/2}Nb_{1/2})O_3$ -$PbTiO_3$ Solid Solution," Journal of Electronic Materials **45**, 6005–6011 (2016).

[19]C. Elissalde and J. Ravez, "Ferroelectric ceramics: Defects and dielectric relaxations," Journal of Materials Chemistry **11**, 1957–1967 (2001).

[20]G. F. Nataf, O. Aktas, T. Granzow, and E. K. Salje, "Influence of defects and domain walls on dielectric and mechanical resonances in $LiNbO_3$," Journal of Physics: Condensed Matter **28**, 015901 (2016).

[21]A. Pramanick, A. D. Prewitt, J. S. Forrester, and J. L. Jones, "Domains, domain walls and defects in perovskite ferroelectric oxides: A review of present understanding and recent contributions," Critical Reviews in Solid State and Materials Sciences **37**, 243–275 (2012).

[22]B. Akkopru-Akgun, *The Role of Defect Chemistry in DC Resistance Degradation of Lead Zirconate Titanate Thin Films*, Ph.D. thesis (2019).

[23]Q. Kim, R. Somoano, C. Lowe Ma, L. B. Coleman, and A. Moopen, "Studies of defects in improper ferroelectrics," Ferroelectrics **36**, 435–438 (1981).

[24]G. E. El-Falaky, O. W. Guirguis, and N. S. Abd El-Aal, "A.C. conductivity and relaxation dynamics in zinc–borate glasses," Progress in Natural Science: Materials International **22**, 86–93 (2012).

[25]E. Sapper, R. Dittmer, D. Damjanovic, E. Erdem, D. J. Keeble, W. Jo, T. Granzow, and J. Rödel, "Aging in the relaxor and ferroelectric state of Fe-doped (1-x)$(Bi_{1/2}Na_{1/2})TiO_3$-x$BaTiO_3$ piezoelectric ceramics," Journal of Applied Physics **116**, 104102 (2014).

[26]L. Zhang, E. Erdem, X. Ren, and R.-A. Eichel, "Reorientation of $(Mn''_{Ti}-V^{\bullet\bullet}_{O})$ defect dipoles in acceptor-modified $BaTiO_3$ single crystals: An electron paramagnetic resonance study," Applied Physics Letters **93**, 202901 (2008).

[27]R. A. Eichel, P. Erhart, P. Träskelin, K. Albe, H. Kungl, and M. J. Hoffmann, "Defect-dipole formation in copper-doped PbTiO3 ferroelectrics," Physical Review Letters **100**, 1–4 (2008).

[28]P. Erhart, R. A. Eichel, P. Träskelin, and K. Albe, "Association of oxygen vacancies with impurity metal ions in lead titanate," Physical Review B - Condensed Matter and Materials Physics **76**, 1–12 (2007).

[29]H. Schmid and L. A. Petermann, "Dielectric constant and electric resistivity of copper chlorine boracite, $Cu_3B_7O_{13}Cl$ (Cu-Cl-B)," phys. stat. sol. (a) **41**, K147 (1977).

[30]E. A. Eliseev, A. N. Morozovska, G. S. Svechnikov, V. Gopalan, and V. Y. Shur, "Static conductivity of charged domain walls in uniaxial ferroelectric semiconductors," Physical Review B **83**, 1–8 (2011).

[31]S. Liu, F. Zheng, N. Z. Koocher, H. Takenaka, F. Wang, and A. M. Rappe, "Ferroelectric domain wall induced band gap reduction and charge separation in organometal halide perovskites," Journal of Physical Chemistry Letters **6**, 693–699 (2015).

[32]G. F. Nataf, M. Guennou, J. M. Gregg, D. Meier, J. Hlinka, E. K. Salje, and J. Kreisel, "Domain-wall engineering and topological defects in ferroelectric and ferroelastic materials," Nature Reviews Physics **2**, 634–648 (2020).

[33]B. A. Connor, R. W. Smaha, J. Li, A. Gold-Parker, A. J. Heyer, M. F. Toney, Y. S. Lee, and H. I. Karunadasa, " Alloying a single and a double perovskite: a Cu +/2+ mixed-valence layered halide perovskite with strong optical absorption ," Chemical Science **12**, 8689–8697 (2021).

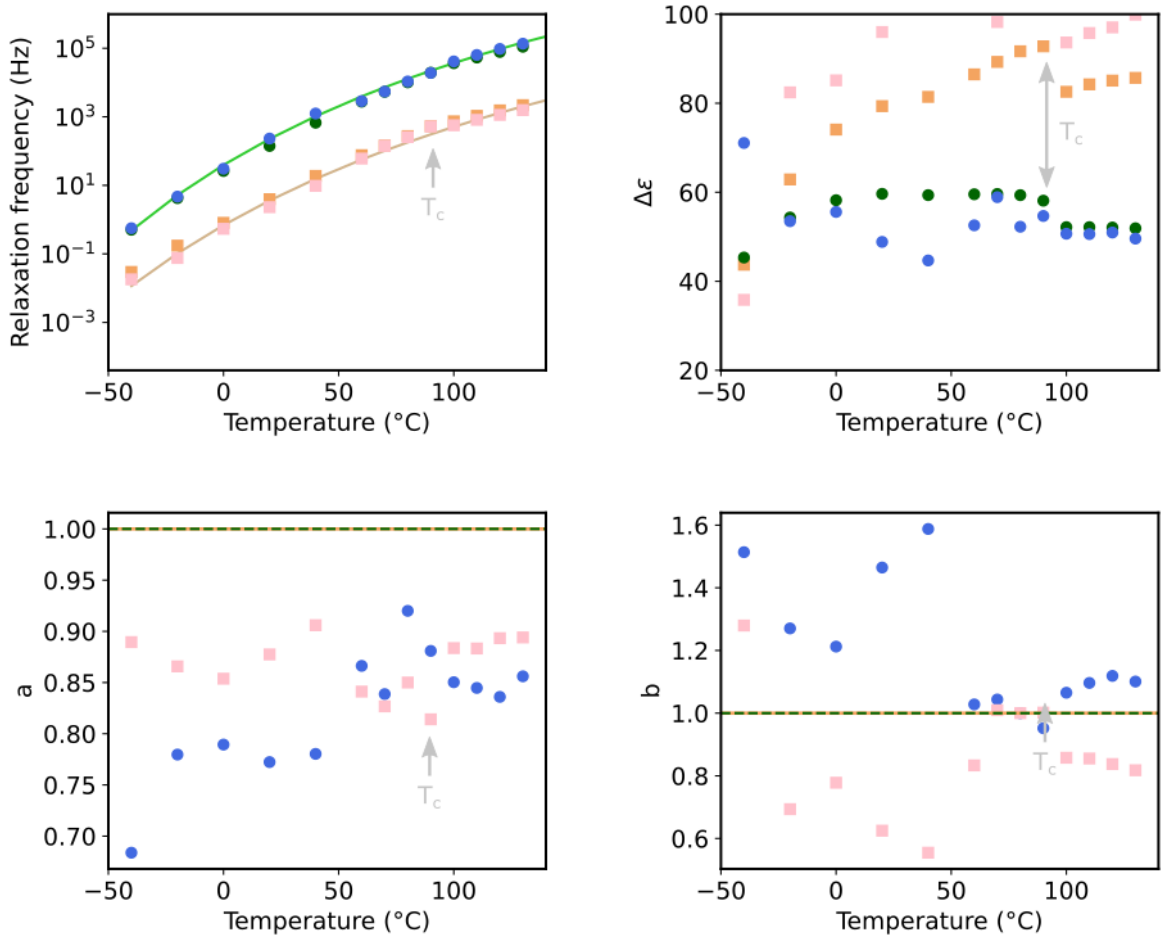

Figure 5. Comparison Havriliak-Negami (HN) and Debye fit. Havriliak-Negami fitting function
$\varepsilon^* = \frac{\Delta\varepsilon_1}{[1+i(f/f_{r,1})^a]^b} + \frac{\Delta\varepsilon_2}{[1+i(f/f_{r,2})^a]^b} + \frac{\sigma}{\varepsilon_0(i2\pi f)^n} + \varepsilon_\infty$
The difference between HN and Debye is with the exponents a and b, which describe the broadening and asymmetry of the relaxation peak respectively. Under the assumptions for a Debye relaxation $a = b = 1$. The relaxation frequencies, amplitudes and the two exponents a and b are presented in this figure. In squares, the high frequency relaxation and in circles, the low frequency one. Green and yellow correspond to the Debye fit while pink and blue represents HN. The difference between the two fits is quite small besides from the a and b exponent. We can notice also a small reduction in the noise of the relaxation amplitudes.

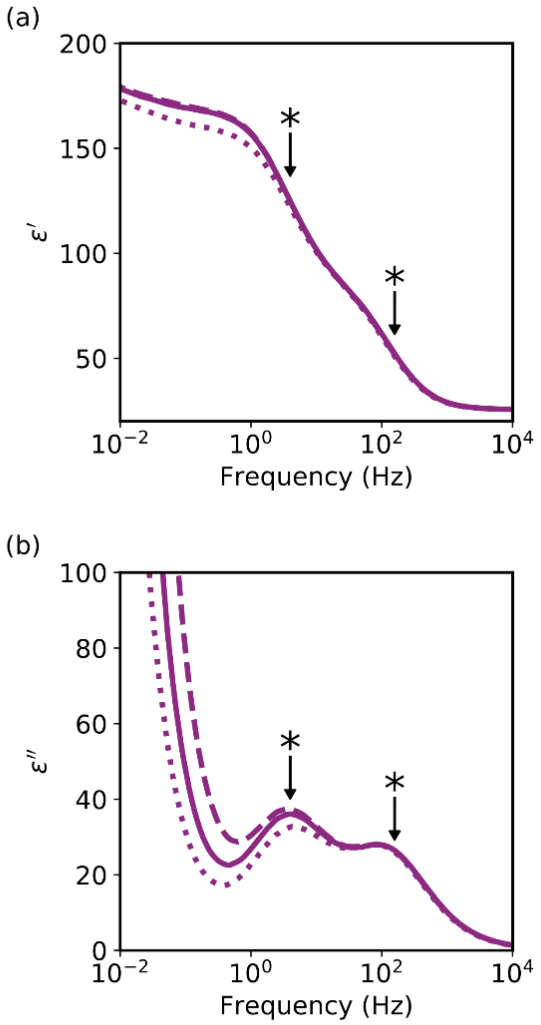

Figure 6. Influence of run cycle on the dielectric relaxations The (a) real and (b) imaginary part of the permittivity are presented before any cooling cycle (dashed line), after cooling at -140 °C (full line) and after heating at 150 °C (dotted line)

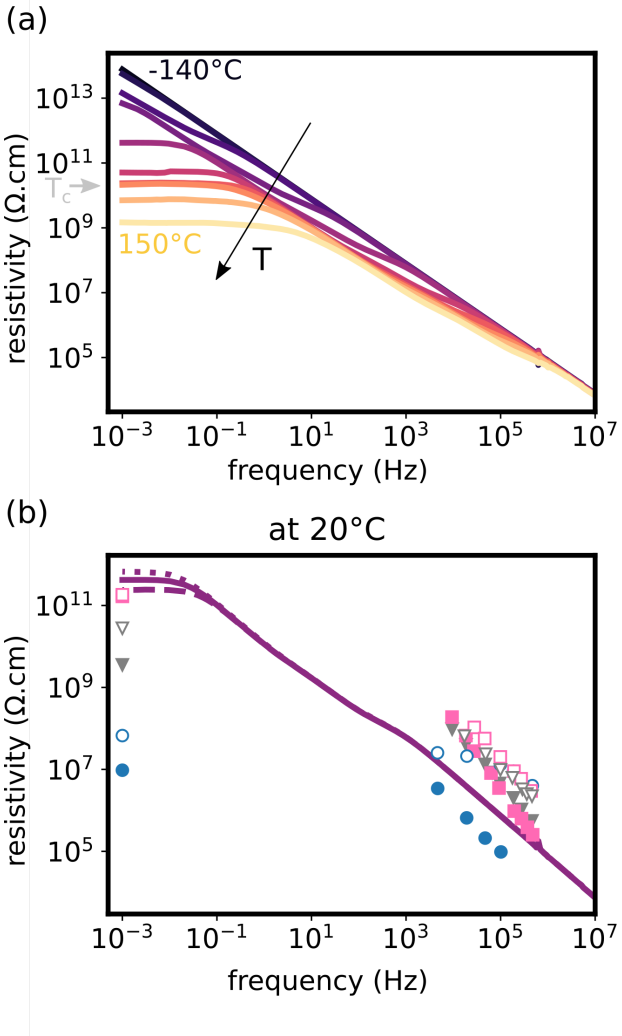

Figure 7. Frequency dispersion of resistivity (a) For different temperatures. It can be seen that at high temperature the resistivity plateaus at low frequencies indicating that the value is the DC value. (b) At 20 °C , for different samples and thermal history. The lines represent our measurements on the same sample after different thermal treatment: before any cooling cycle (dashed line), after cooling at -140 °C (full line) and after heating at 150 °C (dotted line) Symbols represent measurements reported by Schmid and Peterman[29] on different samples and domain configurations (open symbols correspond to single domain measurements)